Lawrence Berkeley National Laboratory
Lawrence Berkeley National Laboratory

Title
IMPEDANCE OF A BEAM TUBE WITH ANTECHAMBER

Permalink
https://escholarship.org/uc/item/7sr1d95v

Author
Barry, W.

Publication Date
1986-08-01

eScholarship.org Powered by the California Digital Library
University of California

LBL-21389
ESG-17

IMPEDANCE OF A BEAM TUBE WITH ANTECHAMBER*

W. Barry, G.R. Lambertson and F. Voelker

Lawrence Berkeley Laboratory
University of California
Berkeley, CA 94720

August 1986

*This work was supported by the Office of Basic Energy Sciences of the U.S. Department of Energy, under Contract No. DE-AC03-76SF00098.

IMPEDANCE OF A BEAM TUBE WITH ANTECHAMBER*

W. Barry, G. R. Lambertson and F. Voelker
Lawrence Berkeley Laboratory
University of California, Berkeley, CA 94720, USA

Introduction

A beam vacuum chamber of the cross section shown in Fig. 1 was proposed[1] to allow synchrotron light to radiate from a circulating electron beam into an antechamber containing photon targets, pumps, etc. To determine the impedance such a geometry would present to the beam, electromagnetic measurements were carried out on a section of chamber using for low frequencies a current-carrying wire and for up to 16 GHz, a resonance perturbation method. Because the response of such a chamber would depend on upstream and downstream restrictions of aperture yet to be determined, the resonance studies were analyzed in some generality. The favorable conclusion of these studies is that the antechamber makes practically no contribution to either the longitudinal or the transverse impedances.

Interpretation of Resonant Modes

A length of this beam chamber with continuing beam tubes attached at the ends forms a cylindrical cavity of not common cross section (Fig. 1). The beam impedances produced by such a cavity may be studied in terms of resonant TM_{nmp} modes. Only those modes having a resonance frequency that is lower than the propagation cutoff frequency of the continuing beam tubes will contribute substantially to the beam impedance. The complexity of considering the many resonances, often overlapping in a long cavity, is reduced if one focuses on the systematics of the real component (Re Z) of impedance averaged over adjacent modes.

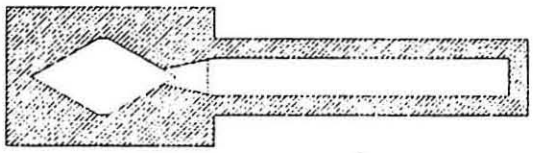

XBL 867-2767

Fig. 1. Cross section of chamber with removable wedge shown dashed in the 1 cm slot.

For a TM mode with axial mode number p, the axial field along the beam centerline of length ℓ is of the form

$$E_z\, e^{j\omega t} = E_o \cos(p\pi z/\ell)\, e^{j\omega t} \quad . \tag{1}$$

At resonance, the peak value of longitudinal impedance is

$$\text{peak } Z_{\parallel}\Big|_{nmp} = RT^2\Big|_{nmp} \tag{2}$$

where R is the cavity shunt impedance and the transit-time factor T is.

$$T = \frac{1}{\ell}\int_{\ell} e^{jk_o z/\beta} \cos(p\pi z/\ell)\, dz \quad . \tag{3}$$

Each mode contributes to the average impedance an area, integrated over $k_o = \omega/c$,

$$\int (\text{Re } Z_{\parallel})\, dk_o = \pi k_o RT^2/2Q \quad . \tag{4}$$

For each mode nmo having p = 0, the associated modes nmp have frequencies given by

$$k_{nmp}^2 = k_{nmo}^2 + (p\pi/\ell)^2 \tag{5}$$

which establishes the density of p-modes as

$$\frac{dp}{dk} = \frac{\ell}{\pi}\left[1 - \left(\frac{k_{nmo}}{k_o}\right)^2\right]^{-1/2} \quad . \tag{6}$$

If we also use the relation, for a long cavity,

$$\frac{R}{Q}\Big|_{nmp} = \frac{R}{Q}\Big|_{nmo}\left(\frac{k_{nmo}}{k_{nmp}}\right)^3 \times \begin{cases} 1 & \text{for } p = 0 \\ 2 & \text{for } p \geq 1 \end{cases} \tag{7}$$

then the local average Re $Z_{\parallel}$ from all modes having indices nm is

$$\text{average Re } Z_{\parallel}\Big|_{nm} = \text{area} \times \text{mode density}$$

$$= \frac{R}{Q\ell k}\Big|_{nmo} \frac{2}{\beta^2\left[1 + \left(\frac{k_o}{\beta\gamma k_{nmo}}\right)^2\right]^2\left[1 - \left(\frac{k_{nmo}}{k_o}\right)^2\right]^{1/2}} \tag{8}$$

The quantity $R/Q\ell k$ for mode nmo is fixed by only the shape and size of the cylinder cross section and is not a function of length. Thus, each TM_{nm}-series contributes an average real part of the impedance given by Eq. (8) starting at k_{nmo} and extending to cutoff of the attached pipes. Also, using the Kramers-Kronig relation,[2] we can find the contribution of the nm-series to Im $Z_{\parallel}$ well below k_{nmo} to be

$$\text{Im } Z_{\parallel} = \frac{R}{Q\ell k^2}\Big|_{nmo} k_o \frac{4}{\pi} \cos^{-1}\frac{k_{nmo}}{k_c} \tag{9}$$

where $k_c = \omega/c$ at cutoff of the attached beam tubes. Therefore the quantities $R/Q\ell k$ for the modes with p = 0 characterize the longitudinal impedance.

From the definition of transverse impedance (x-direction),

$$Z_x = \frac{j}{I_o}\frac{d}{dx}\left(\frac{\Delta p_x c}{e}\right) , \tag{10}$$

the relation to TM modes is not at first apparent, but using the electromagnetically required condition[3] that

$$\frac{\partial}{\partial t}(\Delta p_x) = -\frac{\partial}{\partial x}\ (\text{particle energy}) \tag{11}$$

one can show that at resonance

*This work was supported by the Office of Basic Energy Sciences of the U.S. Department of Energy under Contract No. DE-AC03-76SF00098.

$$\text{peak } Z_\perp = \frac{T^2}{4k_o R}\left(\frac{dR}{dx}\right)^2 \qquad (12)$$

in which $R = (E_o \ell)^2/2P$ as before but now is explicitly a function of x through the dependence of E_o on position, at constant power P.

The average transverse impedance follows from Eq. (12) as in the case of $Z_\parallel$, yielding results of the forms (8) and (9) but with

$$\left.\frac{1}{4Q\ell k_o^2 R}\left(\frac{dR}{dx}\right)^2\right|_{nmo}$$

in place of

$$\left.\frac{R}{Q\ell k_o}\right|_{nmo}.$$

Measurements of Resonances

The quantities $R/Q\ell k_o$ and $(dR/dx)^2/4Q\ell k_o^2 R$ were measured for $p = 0$ TM modes using the perturbation technique to be described. The model was made relatively short (5 cm) in the z direction in order to reduce the number of $p \neq 0$ modes and to increase the sensitivity of the perturbation measurements. A provision for isolating the beam tube from the antechamber was included in the model (see Fig. 1) so that antechamber effects on the impedance of the beam tube alone could be clearly identified.

The perturbation technique for measuring $R/Q\ell k_o$ and $(dR/dx)^2/4Q\ell k_o^2 R$ is based on the Slater perturbation theorem[4] which relates the shift of resonant frequency to the change of stored electric and magnetic energies when a small perturbing object is introduced into the interior of the cavity. That relation is

$$\frac{\Delta f}{f_o} = \frac{\alpha(\Delta U_H - \Delta U_E)}{2U_T} \qquad (13)$$

where

α = shape factor

ΔU_H = magnetic energy in volume of perturbing object

ΔU_E = electric energy in volume of perturbing object

U_T = total energy in cavity

f_o = unperturbed resonant frequency

Δf = shift in resonant frequency

By using the field definitions for electric and magnetic energy in conjunction with Eq. (13) it is possible to determine the quantities $R/Q\ell k_o$ and $(dR/dx)^2/4Q\ell k_o^2$ directly. Each of these quantities must be determined for the isolated beam tube and for the beam tube with antechamber. The beam tube situation will be described first.

As can be seen from Fig. 1 the isolated tube is symmetric about the central axis where the beam circulates. At this location, the fields are either all electric or all magnetic for the TM modes. For the electric case ($H = 0$, $R/Q\ell k_o \neq 0$) the quantity $R/Q\ell k_o$ can be determined by perturbing the cavity, with a metallic half sphere of known volume located on an end plate at centerline and measuring the resonant frequency shift. Knowing that the frequency shift is due solely to a change in electric energy, the following may be derived:

$$\frac{R}{Q\ell k_o} = \frac{-2\ell\eta\Delta f}{k_o^2 \alpha_e \Delta V_m f_o} \qquad (14)$$

where

$\eta = 120\pi$ ohm

$\alpha_e = 3$ (electric shape factor)

ΔV = volume of metal half sphere

Similarly for modes in which $E = 0$ on center and knowing $dE/dx \propto H$ the transverse equation can be derived:

$$\frac{1}{4Q\ell k_o^2 R}\left(\frac{dR}{dx}\right)^2 = \frac{2\ell\eta\Delta f}{k_o \alpha_h \Delta V_m f_o} \qquad (15)$$

where

$\alpha_h = 3/2$ (magnetic shape factor)

In the transverse case the two possible sets of modes are excited by an axial antenna probe displaced from the beam center in either the horizontal or vertical direction. The longitudinal modes are excited by the same antenna located at the beam center.

When the antechamber is present the geometry is no longer symmetric about the beam center, therefore E and H are present simultaneously at this point. Because longitudinal impedances are proportional to E and transverse impedances are proportional to H care must be taken to separate E and H effects when making the perturbation measurements. In the longitudinal case, a dielectric half sphere (teflon) is used to perturb the E field and thus electric energy only. The resulting longitudinal equation is:

$$\frac{R}{Q\ell k_o} = \frac{-2\ell\eta(\epsilon+2)\Delta f_d}{k_o^2(\epsilon-1)\alpha_e \Delta V_d f_o} \qquad (16)$$

where

ϵ_r = dielectric constant of half sphere = 2.1

ΔV_d = volume of dielectric half sphere

$\alpha_e = 3$

Δf_d = frequency shift from dielectric

For the transverse case two separate measurements must be made because there is no magnetic equivalent to a pure dielectric. A metal half-sphere is used to determine $\Delta U_H - \Delta U_E$ and a dielectric half sphere is used to determine ΔU_E. ΔU_H may then be inferred from the two measurements the final result for the transverse case being:

$$\frac{1}{4Q\ell k_o^2 R}\left(\frac{dR}{dx}\right)^2 = \frac{2\ell\eta}{k_o f_o}\left[\frac{\Delta f_m}{\alpha_h \Delta V_m} - \frac{(\epsilon+2)\Delta f_d}{(\epsilon-1)\alpha_e \Delta V_d}\right] \qquad (17)$$

where

$\alpha_h = 3/2$

$\alpha_e = 3$

Thus Eqs. (14) through (17) enable one to measure $R/Q\ell k_o$ and $(dR/dx)^2/4Q\ell k_o^2 R$ in all cases.

In practice, the size of the perturbing half sphere must be small enough so that the fields may be considered uniform across it. At the same time the half sphere must be large enough to produce a measurable shift in resonant frequency. For a single size of half sphere both of these conditions can be met at low frequencies. However at higher frequencies the half sphere becomes too large. For all frequencies, metal and dielectric half spheres of size

large enough to produce relative frequency shifts of ~ .2% were used. To improve the accuracy at high frequencies the half spheres were calibrated using a circular cylindrical cavity with known modes. An effective volume for each half sphere was then computed and used for the ALS chamber measurements.

The first measurement made was a broadband sweep (0-16 GHz) of the 5 cm cavity model so that all of the p = 0 modes could be identified. By changing the probe position in the x and y directions the modes could be further identified as primarily longitudinal, horizontal or vertical. Using the techniques described above, $R/Q\ell k_0$ was measured for the beam chamber with and without the antechamber, the results appear in Fig. 2. Also contained in Fig. 2 are calculated $R/Q\ell k_0$ for a 5.5 cm x 4.2 cm rectangular cross section to provide a reference. It can be seen that the isolated beam tube behaves approximately like the rectangle.

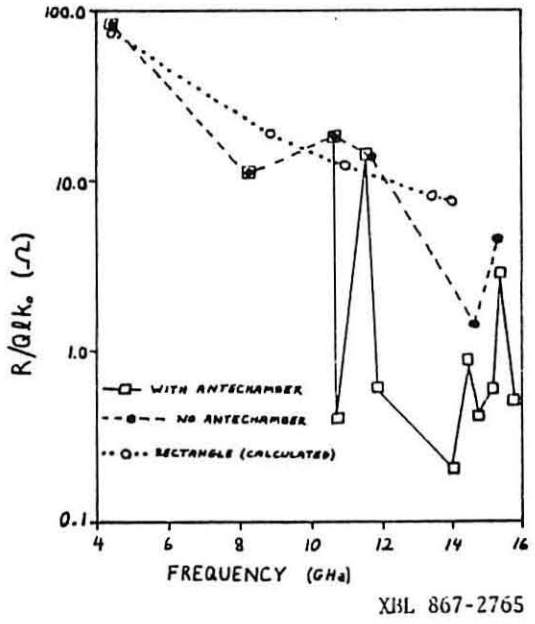

XBL 867-2765

Fig. 2. Longitudinal modes with p = 0

New modes introduced by the antechambers are all above 10 GHz and have considerably lower $R/Q\ell k_0$ values. Only above 14.5 GHz do the added modes become of significant relative magnitude. The interpretation of these modes as being a transition from the small beam tube to a larger cylinder at about 15 GHz is illustrated in Fig. 3, in which the cumulative values of $R/Q\ell$ are shown for a calculated rectangle and for the beam chamber with and without antechamber. It is characteristic of simple cylinders that these sums fall along a line of slope $\eta/2\pi$ = 60 ohm; presence of the antechamber does not cause a departure from that pattern.

Figures 4 and 5 show measurements of $(dR/dx)^2/4Q\ell k_0^2 R$ without and with the antechamber. Again no low-frequency modes are added by the antechamber and changes at high frequency would not cause a signficant change in average transverse impedances.

Measurements with a Wire

The reaction of the beam chamber to a current-carrying wire was measured to search for any low-frequency resonances or reactive impedance below the 4.5 GHz cutoff frequency of the beam tube alone. To reduce distortion of the test chamber's response by the wire, one desires a wire of small diameter and hence of higher TEM impedance, $Z_{\parallel}$, than the conventional 50 ohms of the network analyzer terminals. We fabricated coaxial

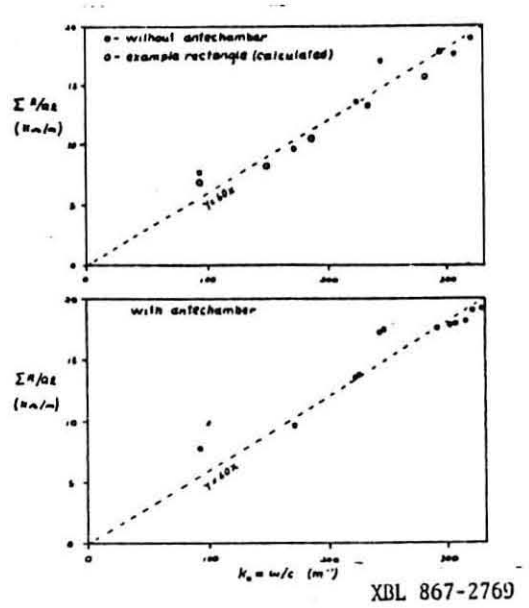

XBL 867-2769

Fig. 3. Cumulated $R/Q\ell$ values

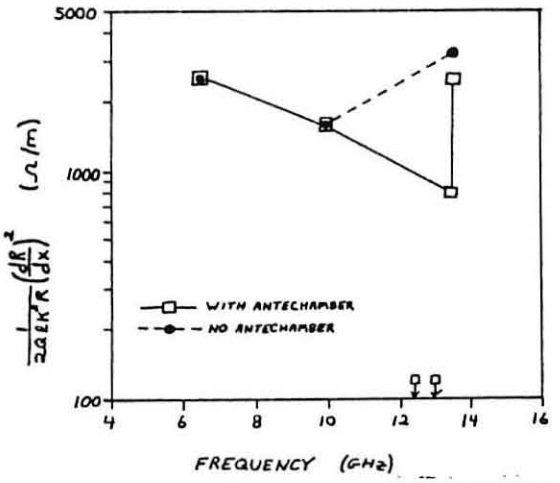

XBL 867-2770

Fig. 4. Strengths of horizontally-coupling modes.

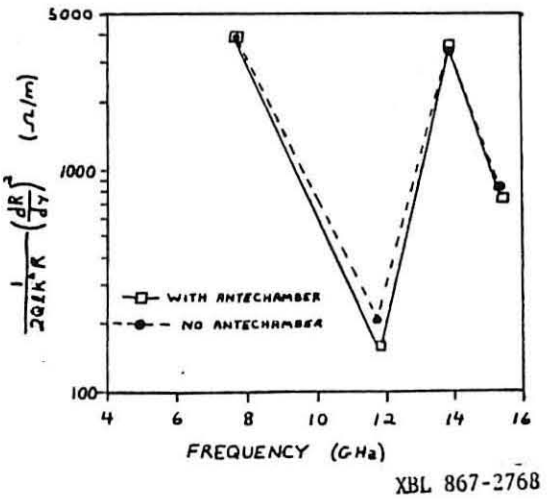

XBL 867-2768

Fig. 5. Strengths of vertically-coupling modes

Chebyshev tapers to transform from 7 mm connectors to 162.5 ohm in a larger circular aperture. These tapers and adapters from circular to diamond cross section (see Fig. 6) were made by electroforming a thick copper layer onto precision mandrels of aluminum. The mandrel was then dissolved by sodium hydroxide. With a carefully-fitted wire the return loss from reflections and mismatch in the total assembly shown in Fig. 6 was reduced to less than -24 dB from 0.6 to 5 GHz, and was -29 dB over much of that range. Performance of this hardware was checked by measuring the TM_{010} resonance of a circular cavity of known characteristics.

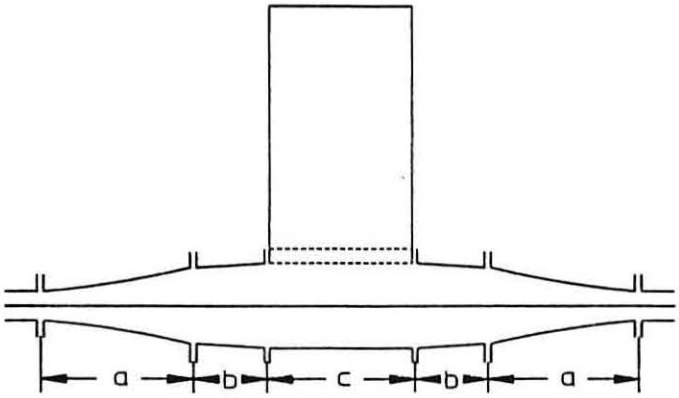

Fig. 6. Wire setup: (a) 45-cm taper transformers, (b) transitions to diamond shape, (c) 15-cm section of chamber with antechamber.

With reflections adequately reduced, the beam impedance is given by

$$Z_{\parallel} = 2Z_W\left(1-S_{21}\right) - R_c$$

where R_c is a correction for resistive losses in the wire. For detecting any effect of the antechamber, it was simple to interpret the change in S_{21} produced by removing the wedge plug between beam tube and antechamber.

In Fig. 7, the magnitude of S_{21} with and without antechamber are shown superposed. The broadening of the trace above 3 GHz is the only evidence of an effect of the antechamber. (The spike at 3.7 GHz was on the tube-only trace and appeared to be spurious.) Any added impedance is therefore less than the instrumental resolution; e.g., 0.4 reactive ohm at 2 GHz. The length of the test section was 22.4 cm.

Twin wires were used to measure horizontal and vertical impedances[5] but less care was taken to reduce reflections. Results for the two conditions showing perfect retrace are given in Fig. 8. Reflections in hybrids used to drive the twin conductors in opposing phase produce the periodic waves in S_{21}. Nevertheless, one can see that no detectable change arises from addition of the antechamber. In this case the effect must be less than 2500 Ω/m.

Conclusions

The small beam tube with slot-isolated antechamber responds as a small cylinder up to the frequency (~ 15 GHz) where energy can propagate transversely in the narrow slot. The important function of the slot is to prevent the beam from coupling to the many lower-frequency modes of the antechamber. Therefore the beam impedances are those of the small cylinder connected to continuing chambers of other cross sections; those impedances may be calculated from the measured values of $R/Q\ell k$ and $(dR/dx)^2/4Q\ell k^2R$ for those TM modes that are below cutoff of the continuing chambers. If that frequency were higher than the

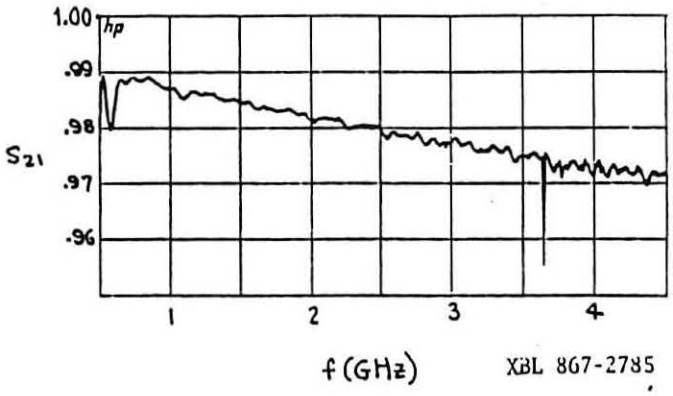

Fig. 7. Superposed responses of single wire with and without antechamber

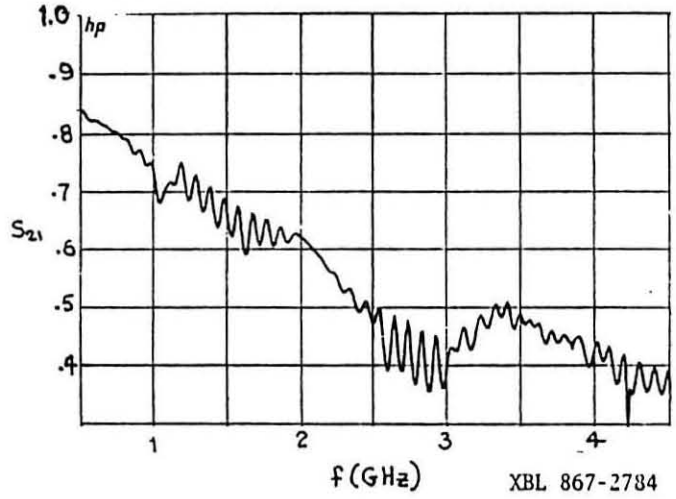

Fig. 8. Superposed responses of twin wires with and without antechamber

slot-coupling at 15 GHz, only an increased density of modes is expected, with little change in average beam impedances as indicated by Fig. 3.

One may assume that the shape of the antechamber is not important, permitting one to vary its shape or insert objects as long as the slot has appreciable transverse depth and smooth cylindrical geometry is maintained in the slot and the beam tube.

References

1. NCAM Conceptual Design Report, Vol. 1, Lawrence Berkeley Laboratory, Berkeley, CA (1983), p.3-28.

2. J.D. Jackson, Classical Electrodynamics, Second Edition, Wiley, New York (1975), p.311.

3. G.R. Lambertson, "Dynamic Devices," 1985 U.S. Summer School on High-Energy Particle Accelerators, to be published.

4. J.C. Slater, Microwave Electronics, Van Nostrand, Princeton, NJ (1950), p. 81.

5. G. Nassibian and F. Sacherer, "A Method for Measuring Transverse Coupling Impedance," CERN/ISR-TH/77-61 (1977).